IV. Department of Engineering and Technical Services

The Department of Engineering and Technical Services is involved in the design, fabrication, construction and operation of experimental devices in the fields of software and hardware.

This department is composed of engineers, and their tasks fall under the following five goals:

1) To develop advanced and systematic engineering capabilities on the basis of basic engineering results which have been obtained thus far.
2) To educate excellent engineers with responsible administration.
3) To cultivate creative engineering abilities.
4) To improve the documentation of and the transfer of engineering knowledge to the next generation.
5) To perform tasks with a systematic responsibility.

The department consists of the following five divisions: the Fabrication Technology Division takes care of the construction of small devices and the quality control of parts for all Divisions. The Device Technology Division is responsible for LHD and LHD peripheral devices except for heating devices and diagnostic devices. The Plasma Heating Technology Division has responsibility for the ECH system, the ICRF system, and the NBI system. The Diagnostic Technology Division develops, operates and maintains all diagnostic devices and the Control Technology Division has responsibility for the central control system, the cryogenic system, the current control system and the NIFS network. The number of staff is 46 engineers and 12 part-time workers. We take care of the development, the operation and the maintenance of LHD and the LHD peripheral devices with about 46 operators.

1. Fabrication Technology Division

The main work of this division is the fabrication of experimental equipment. We also take care of technical consultation and experimental parts supplies to persons concerned with the LHD experiment. In addition we handle the administrative procedures of the department.

An electron beam welding machine is installed in the Central Workshops, in this fiscal year(FY).

The number of machined requests is 216 cases, and the production parts total number is 1,022 in this FY. And for electronic engineering, these are 13 and 49. The details of some activities are as follows.

(1) The mirror control circuit for ECRH

The basic part of the mirror control circuit for ECRH was made as shown in Figure 1. The principal part of the circuit is constructed of the FPGA (Field Programmable Gate Array) device. This circuit embeds the Linux micro-computer. Thus it can control the mirror position remotely through the Ethernet LAN. It has AD/DA converters and digital IOs, so that, it can measure and set the mirror position.

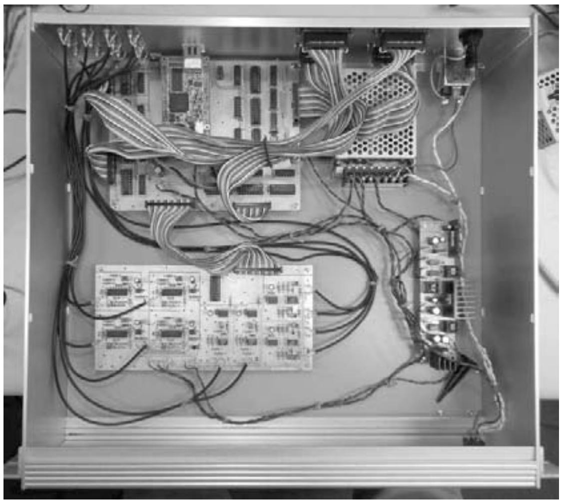

Fig. 1. The mirror control circuit for ECRH.

(2) The multi-channel isolation amplifier

The 8 channel isolation amplifier with both characteristics DC to 1MHz frequency and 500V isolation between input and output was made as shown in Figure. 2. The toroidal power transformers are used to minimize interference between channels. The operation test of the amplifier will be taken at the GAMMA10 at the University of Tsukub.

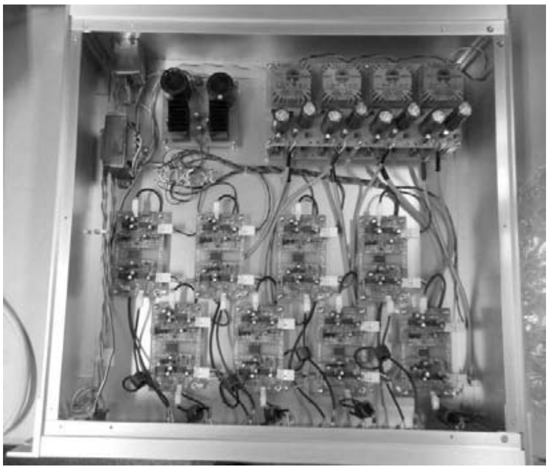

Fig. 2. The multi-channel isolation amplifier.

(3) 2.5 inch corrugated miter bend for microwave at the frequency of 28 GHz

The corrugated miter bend is a component of the vacuum waveguide system that is installed in the part of the 90 degrees bend. In order to improve the transmission efficiency of 2.5inch-corrugated waveguide, it is necessary to cut corrugated slots on the surface of the inside diameter of the miter bend. Parameters of the rectangular corrugation are width 2.5mm and 1.9mm depth, periodic length 4.6mm.

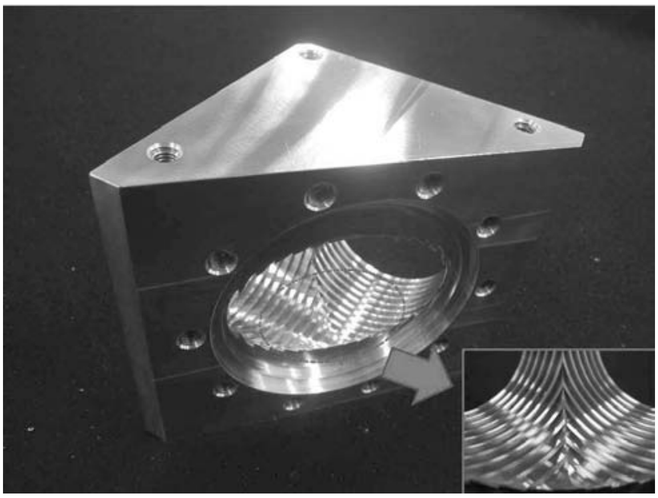

Fig. 3. Corrugated miter bend.

(4) Notch filter

This notch filter (as shown in Figure. 4) is a part of the receiver for the Thomson scattering measurement. It is planned to remove high frequency noise from the 77GHz gyrotron. The size is 20mm width, 20mm height and 50mm length. The size of the waveguide's mouth is 3.098mm width, 1.55mm height and the same length. It is made of anoxia copper by two parts using screws to put it together. The waveguide have two grooves of 1mm width, 0.5995mm depth and 2.5mm length, located 1.975mm and 5.925mm away from the center. We use the machining center and the general-purpose lathe to make this.

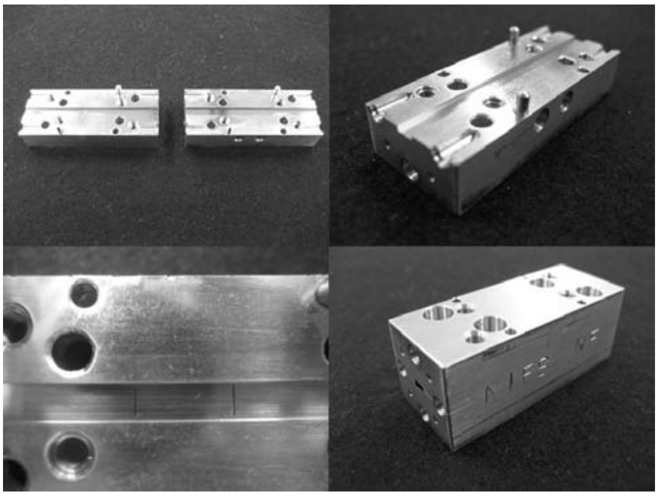

Fig. 4. Notch filter.

2. Device Technology Division

The Division supports the operation, the improvement and the maintenance of LHD.

(1) Operation of LHD

We started to evacuate the air from the cryostat vessel for cryogenic components on August 12, 2013 and the plasma vacuum vessel on August 13. Subsequently, we checked air leaks from maintained flanges of the plasma vacuum vessel. The number of those checked flanges was 125. As a result, we found four leaked places and repaired them. The pressure of the plasma vacuum vessel was achieved below $1x10^{-5}$ Pa on August 26 and the pressure of the cryostat vessel was achieved the adiabatic condition ($< 2x10^{-2}$ Pa) on August 14.

The LHD experiment of the 17th experimental campaign began on October 2 and ran through December 25. The number of days of the plasma experimental period was 52 days in total.

During this experimental campaign, our vacuum pumping systems were able to evacuate the air from both of the vessels without trouble. The LHD operation was completed on January 17, 2014.

(2) Design of the gas supply system

The LHD experiments using deuterium will start in 2016. The current gas supply system with a gas puffing device is simple and multifunctional, but the system must be drastically redesigned for the experiments using deuterium. The new gas supply system will supply hydrogen, deuterium, helium (impurity densities of these are under 100ppb), argon, neon, nitrogen and so on (impurity densities of these are under 100ppm) as the fuel gases. They are available to 8 MPa of gas pressure. The gas puffing device and the pellet injection device are the utility systems to inject the fuel gas into LHD. We designed a new system to supply the fuel gas to these utility systems with high quality and pressure.

(3) The thermal analysis of the cryo-sorption pump in the closed helical divertor

For improvement of the particle pumping efficiency, there are in-vessel cryo-sorption pumps and a baffle structure which consists of the divertor plates and the dome structure made from the isotropic graphite, as illustrated in Figure.5, in the closed helical divertor (CHD) region.

It was evaluated that the thermal performance of the shield structure (the liquid-nitrogen: LN_2 shield and the water shield) is adequate to protect the cryo-panel from the radiation heat flux due to the divertor plates in 2012.

The heat load to the cryo-panel in the cryo-sorption pump has been checked. The heat load to the cryo-panel is divided into four classes, (a) the radiant heat from the LN_2 shield: q_c, (b) the heat transfer from support parts: q_s, (c) the heat of adsorption of H_2 gas: q_{g1}, and (d) the heat transfer through H_2 gas: q_{g2}. The result of this thermal analysis is shown in Table 1. It is revealed that the heat load due to the H_2 gas adsorption is dominant when the H_2 pellet is injected at 10 Hz in the vacuum vessel of the LHD. At this time, the temperature of the base plate in the cryo-panel is approximately 15 K. It is necessary that the temperature of the activated carbon is under 20 K in order to keep the efficient pumping property. Therefore, the numerical analysis using the finite element method code (ANSYS) was carried out to evaluate the temperature of the activated carbon. The photograph and the simulation model of the cryo-panel are shown in Figure 6 and in Figure 7. The activated carbon is put on the base plate in "scale-like" for the purpose of increasing in the number of the activated carbon put on the base plate. Figure 8 shows the simulation model and the calculated temperature distributions of the cryo-panel. The maximum temperature on the activated carbon is approximately 17 K, and it is the temperature for keeping the efficient pumping property. Therefore, the cryo-sorption pump in the CHD is adequate to pump the H2 gas under the maximum heat load condition.

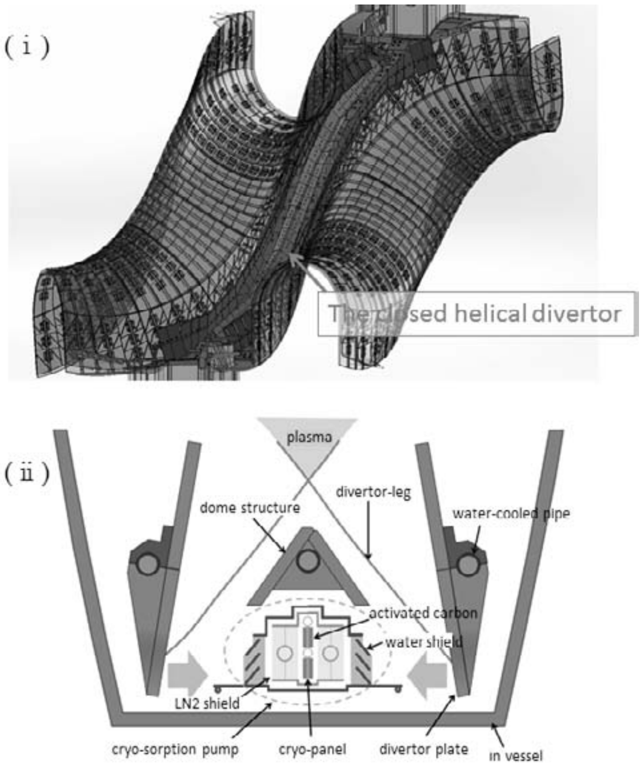

Fig. 5. (i) The schematic view of the vacuum vessel and the closed helical divertor inside the LHD and (ii) the cross-sectional view of the CHD

Table.1. The classes of the heat load to the cryo-panel

Item	Heat Load
(a) The radiant heat from the LN2 shield (W)	1.4
(b) The heat transfer from support parts (W)	8.6
(c) The heat of adsorption for H2 gas (W)	17.5
(d) The heat transfer through H2 gas (W)	0.41

$$(a)\ q_c = \sigma \times \varepsilon \times \left(T_{LN2}^4 - T_p^4\right) \times A$$
$$(b)\ q_s = \lambda_{Cu}\left(T_1 - T_p\right)\frac{A_1}{L_1} = \lambda_{Z_rO_2}\left(T_2 - T_1\right)\frac{A_2}{L_2} = \lambda_{Cu}\left(T_{LN2} - T_2\right)\frac{A_3}{L_3}$$
$$(c)\ q_{g1} = C_p\left(T_g - T_p\right)SP + \lambda SP$$
$$(d)\ q_{g2} = 0.243 \times \frac{\gamma+1}{\gamma-1} \times a_0 \times \left(T_g - T_p\right) \times \frac{P}{\sqrt{MT}} \times A$$

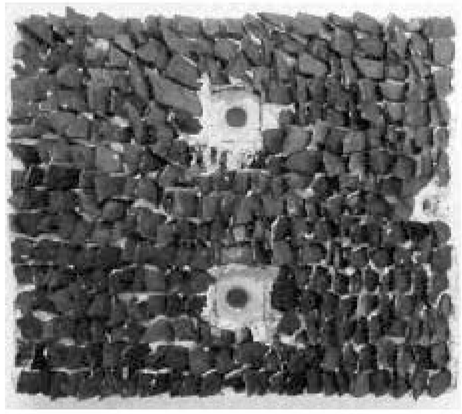

Fig. 6. A photograph of the cryo-panel in which the activated carbon is put on the base plate in scalelike.

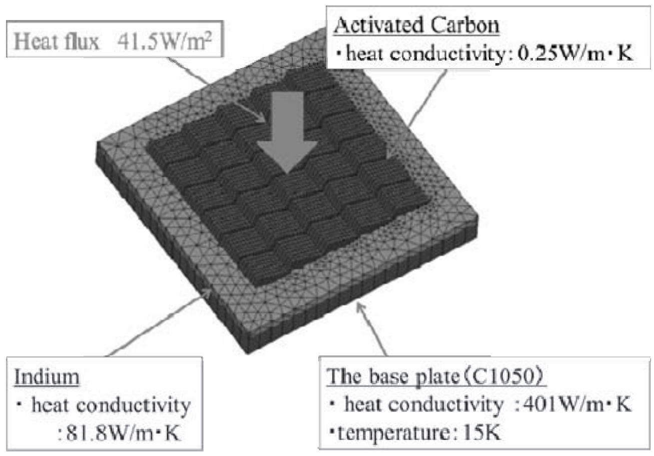

Fig. 7. The simulation model of the cryo-panel

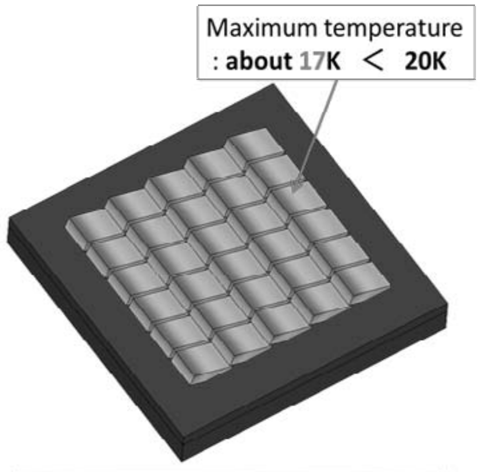

Fig. 8. The temperature distributions of the activated carbon on the cryo-panel.

(4) Development of demand real-time monitoring system

Devices using the LHD experiment consume vast amounts of electricity. Therefore, we monitor power demand not in excess of contract power. We used a demand monitoring web page to monitor power demand. There was one problem, which was that the web page showed 1 minute behind compared to the real-time power demand. This made the control power consumption difficult when power demand was approaching contract power. To cope with the issue, we developed a new system that monitors power demand in real-time. We had started to use the new system and confirmed that this system could monitor the more accurate demand from the monitoring web page.

(5) Development of a movable material probe system at 10.5L-port in LHD

We developed a device (movable material probe system) to irradiate materials to plasma, and installed the device at 10.5L-port in LHD. The system is shown in Figure 9. After irradiation, we could take materials out of this system while keeping high vacuum in LHD. The system could move materials up and down. Maximum slide stroke is 4122mm. The system can also rotate materials from -180 degree to 180 degree. The material holder has thermocouples and heater, and we can heat materials and measure the temperature.

We also developed a control system for the system. It mainly consists of PLC, touch panel and remote control computer.

Because this had been developed by ourselves, we could achieve the reduction of the development cost and ensure the flexibility in the device operation. During the 17th experimental campaign, no trouble or failure was reported.

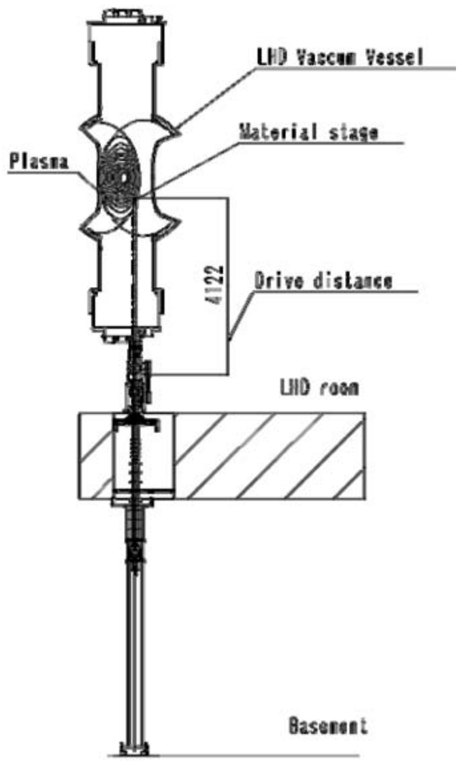

Fig. 9. Movable material probe system.

(6) The test of the radiation gas monitor for the outdoor exhaust pipe

During the fiscal year, we installed the pressurised ionisation chamber for outdoor exhaust pipe of exhausting the gas from LHD to outdoors, and checked whether we could use it as a radiation gas monitor. We found the following as a result of the examination. 1) When the exhaust gas from NBI enters the pressurised ionisation chamber, water accumulates in the chamber and it becomes impossible to get measurement data. 2) Background data are not stable in order to be affected by the change of the radon density in the exhaust gas strongly.

To solve these problems we must examine a remodeling of the chamber and a change to a different radiation monitor.

(7) The tritium sampler system

We monitored the tritium concentrations in the stack by the tritium sampler system. The tritium in the three chemical form is collected as water by this system. The schematic diagram of this system is shown in Figure 10. The amount of the tritium in the collected water is measured by the low background liquid scintillation counter. The result of the measurement date from 2013/4/1 to 2014/3/31 is shown in Figure 11. It was found that the levels of tritium concentration are much lower than the control level in NIFS.

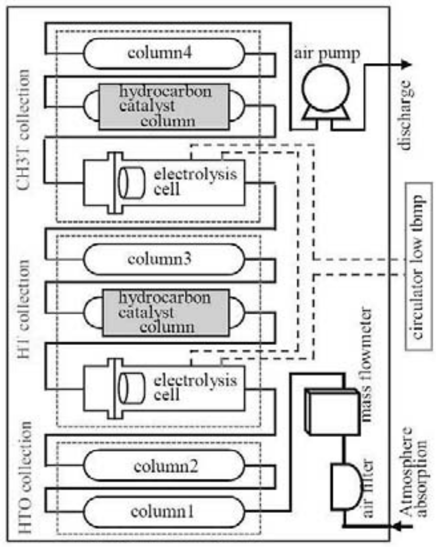

Fig.10. Atmosphere sampling device flow chart.

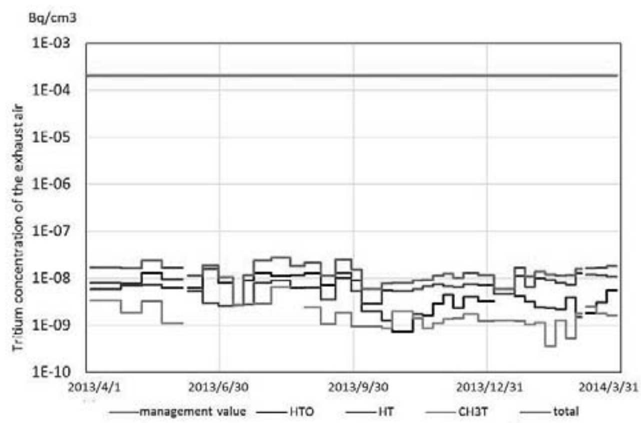

Fig.11. The tritium concentration of the exhaust air

(8) Development of outgas analyzer

A device for analyzing the outgas from material in the vacuum was developed. Figure 12 shows the outgas analyzer that we have developed. Mass analyzer is installed at the top and exhaust system is at the bottom. In addition, a baking heater for material heating is also set up. This device can analyze the outgas from a material in a vacuum of between 1e-5 from 1e-2 Pa. The method is as follows. The outgas data is made from a comparison between a material exist or not. From this result, we obtain the outgas rate of a material. We also obtain the heat characteristic from the comparison of the outgas data which is baking-material and non-baking-material. Until the accomplishment of this outgas analyzer, we conducted the design of this device using CAD, and the development of the software for measuring the vacuum gauge.

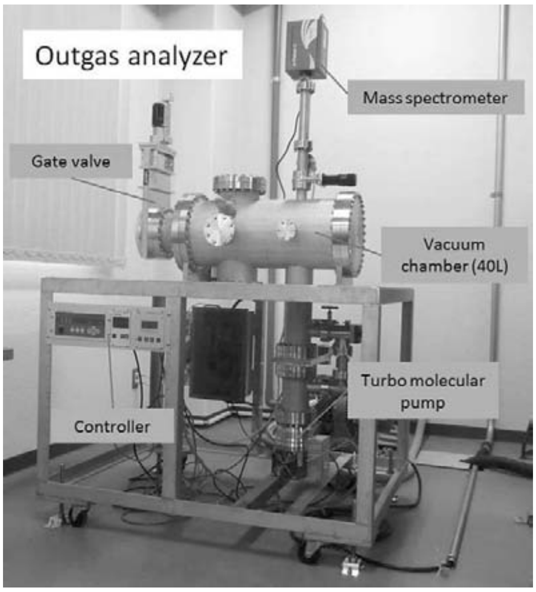

Fig. 12. The outgas analyzer.

2. Plasma Heating Technology Division

The main tasks of this division are the operation and the maintenance of plasma heating devices and common facilities. We have also performed technical support for improving, developing and newly installing these devices.

Two Field-Aligned-Impedance-Transforming (FAIT) antennas for ICRF were newly installed on the 4.5U and L ports of the LHD. The six antennas of LHD in total were operated at the frequency of 38.47MHz during this plasma experiment cycle. Injection power of this device reached 3.2 MW at maximum and 1.3 MW in CW. In ECH, two gyrotrons of the 77(s/n3) and 154 GHz(s/n1) were improved to furnish a sub-window so as to reduce a troublesome stray radiation inside the tube. In the 17th experimental campaign, simultaneous injection power from gyrotrons became about 4.6MW. NBI was stable, and incidence was possible. Total NB injection power reached 27.6MW. The highest ion temperature of 8keV is achieved by NBI. The motor generator (MG) supplied electric power stably and reliably to ECH in addition to NBI. The pure water cooling systems for the heating device were updated by renewing the cooling towers, etc., from January, 2014.

The details of these activities are as follows.

(1) ECH

(a) Gyrotron Operation & LHD experiments

During the 17th experimental campaign, we could maintain the total injection power level that is equal to previous campaign. We injected ECH power stably during the whole campaign without any severe troubles that required a stop of operation for several days to restart. Figure 13 shows the result of ECH injection to LHD in this campaign. The low power injection indicates continuous wave (CW) operation by these gyrotrons, which were improved to attach the relief window and the load absorbing diffracted microwaves in the gyrotron. The improvement highly contributed to the CW experiment, which shows the achievement of an injection of approximately 47minutes by #4 gyrotron.

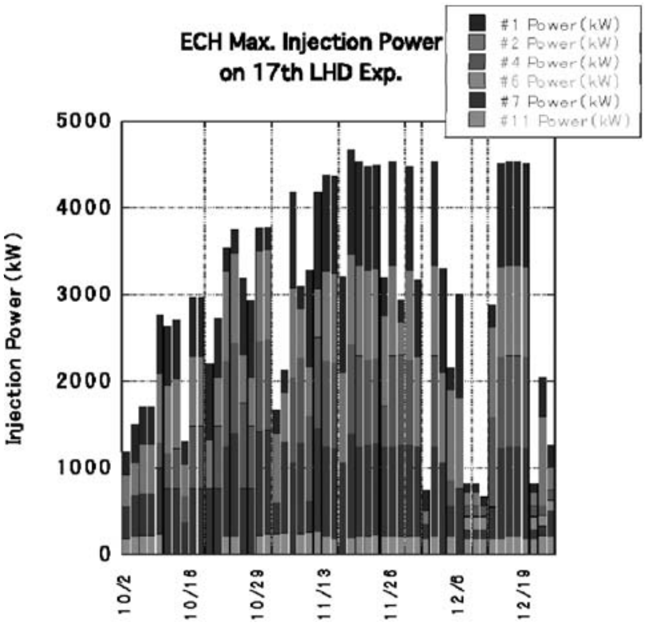

Fig. 13. The history of ECH injection power during the 17th experimental campaign.

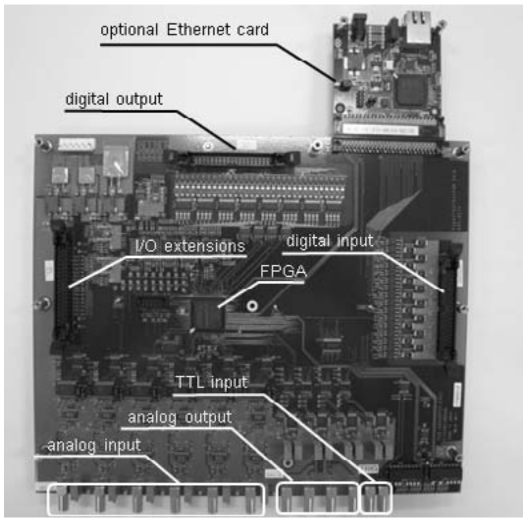

Fig. 14. FPGA board with various I/O channels and optional Ethernet card.

(b) Development of fast mirror control system by FPGA

A board mounted with a field programmable gate array (FPGA) chip has been designed to realize feedback control of the ECH beam position to maintain higher electron temperature by ECH. Figure 14 shows the FPGA board. The heating position is determined by a plasma diagnostic signal related to the electron temperature, such as electron cyclotron emission (ECE) and Thomson scattering.

(c) Improvement in the rotation speed of a polarizer mirrors

Until the 16th experimental campaign, polarizers of max. rotation speed of 2.5deg/s had been installed in 4 transmission lines, and polarizers of max. rotation speed of 12deg/s have been installed in the other 4 transmission lines. Before the 17th experimental campaign, we replaced polarizers of 2.5deg/s with those of 180deg/s. As a result, the problem that the setting of polarizers was not completed between discharges has been resolved. Figure 15 shows the polarizer of max rotation speed of 180deg/s. Also, the polarizers of 12deg/s will be replaced by those of 180deg/s before the 18th experimental campaign.

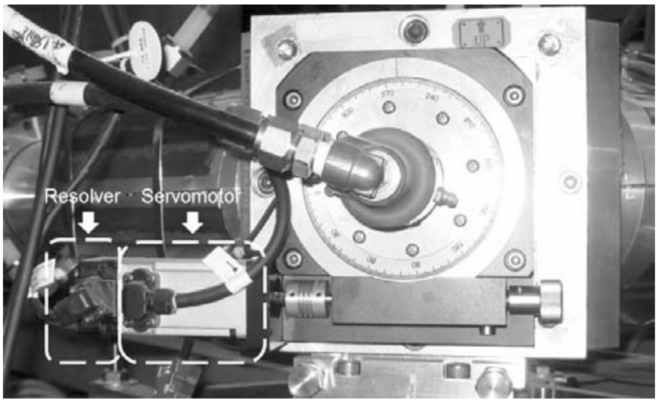

Fig. 15. The polarizer (max rotation speed of 180deg/s). It is intact except for the motor and resolver.

(2) ICH

(a) Operation & LHD experiment

In the 17th experimental campaign, two FAIT Antennas were installed in the 4.5U&L ports of the LHD. Thus, we carried out the LHD experiment in total six antennas with addition to two HAS antennas at the 3.5U&L ports and two Poloidal Array antennas at the 7.5U&L ports. In the 16th experimental campaign, we selected two RF oscillators out of four oscillators from #1 to #4 to connect to the 3.5U&L antennas in consideration of the experiment frequency. However, in the 17th experimental campaign, we decided the combination of an oscillator and an antenna. Then, the oscillators of #1 and #2 were connected to the 3.5U&L antennas and the oscillators of #3 and #4 were connected to the 4.5U&L antennas. The total injection power with the six antennas into the plasma reached about 3.4 MW in the short pulse of 3 seconds at the experiment frequency of 38.47 MHz.

Moreover, we cut and removed the Faraday shield of the 7.5U antenna in order to prevent sparks that occurred in the vicinity of the antenna during a steady state discharge in the 16th experimental campaign.

In the 17th experimental campaign, sparks did not occur, and we carried out a steady state discharge with the six antennas and the injection power into the plasma reached 0.9 MW in the 2860 seconds discharge.

(b) Construction of the transmission lines for 4.5U&L antennas

Although the new antennas were installed in the 4.5U&L ports of LHD and the oscillators were also prepared for them in the Heating Power Equipment Room, most of the transmission lines which connect to them were not installed. We adapted the air-cooling coaxial tube made from the copper rigid pipe of 203 mm in diameter for the transmission lines in the Heating Power Equipment Room, and the water-cooling coaxial tube made from the aluminum rigid pipe of 240 mm in diameter in the other area.

We installed these transmission lines with improvement from the existing transmission line as follows.

i) The water-cooling jacket was attached between the flange of the LHD port and the flange (ICF305) to which the antenna was connected.

ii) The part which can flow cooling water for an outer conductor was added at the connection between a feed-through and a coaxial tube.

iii) A thermocouple was installed for measurement of the surface temperature of a feed-through ceramic in addition to an IR sensor.

iv) The coaxial tubes, which can block the insulation gas between an inner and an outer conductor and the cooling water in an inner conductor, was incorporated into the transmission lines in the Heating Trench.

i) and ii) were carried out because the cause of temperature rise at the feed-through ceramic was considered insufficient cooling of the outer conductor near the feed-through.

iii) and iv) were carried out as a preparation for the deuterium experiment.

Fig. 16. Layout of the six transmission lines in the Heating Trench.

(3) NBI

(a) The operation and maintenance of NBI in the 17th campaign of LHD experiments

In the 17th campaign, approximately 5,000 shots of beams were injected into the LHD plasmas with three negative-NBIs (BL1, BL2, and BL3). The injection history of the total injection power for the negative-NBIs is shown in Figure 17. The maximum injection power in this campaign was 15.1MW, which was almost equal to the designed value of 15MW. As for the positive-NBIs (BL4 and BL5), about 3,000 shots of beams were injected into the LHD plasmas. The maximum injection power of each positive-NBI reached to 6MW.

None of the NBIs had any significant trouble which stopped the LHD plasma experiments, but there were minor troubles. BL1 and BL3 had air leaks in the ion sources. BL2 had a failure of the power supply unit for the VME in the data acquisition system. BL3 had a failure of the mass flow controller for the gas supply into the ion source. BL5 had a failure of the power supply unit in the filament power supply system. These troubles did not lead to serious problems in the plasma experiments owing to speedy and appropriate recoveries.

The NBIs were utilized for most of the LHD plasma experiments and contributed to them throughout the campaign.

To enhance the performance of the LHD plasmas, BL4 has been designed so as to make it possible to inject 60keV-9MW of beams with renewal of the beam line components, the power supply system and the ion sources for several years. This upgrade of BL4 is now under construction.

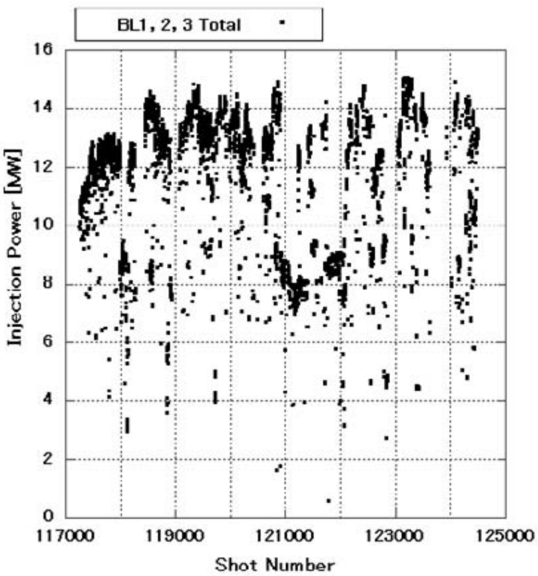

Fig. 17. History of the total injection power for the negative-NBIs.

(b) Upgrade of the data acquisition system in NBI#4

NBI#4 had four ion sources of which the maximum beam energy is 40keV in the 17th experimental campaign. We upgrade the power supply system to increase the beam energy from 40keV to 60keV. Accordingly, we need also upgrade the data acquisition system for NBI#4 because of the increase of signals to be monitored. Therefore, we installed additional hardware and modify the software. See Figure 18.

We started the upgrade of data acquisition system after the 17th campaign and it is currently in progress. We are scheduled to start the operation in October 2014.

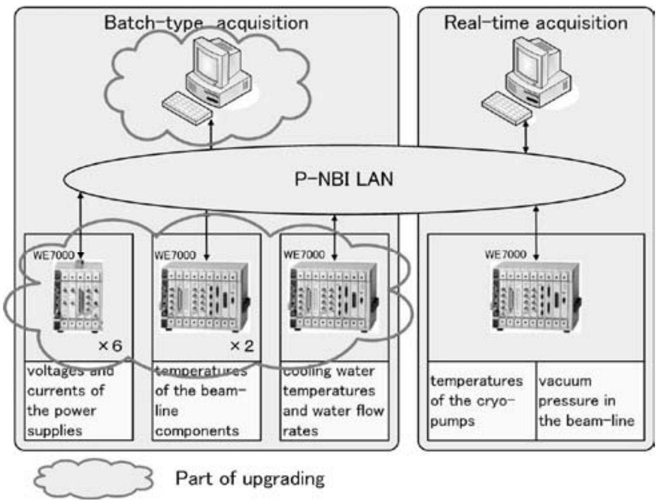

Fig. 18. A schematic diagram for the data acquisition system of NBI#4.

(c) Evaluation of neutral beam injection power

The Neutral Beam (NB) injected power is evaluated from the temperature rises of Calorie-Meter Arrays (CMA), which are consists of Molybdenum chips and are installed in armor tiles at the counter wall of NB injection-port. The temperatures of calorie-meter chips are measured by sheath type thermocouples via isolation amplifiers using the WE data acquisition system. Under weak magnetic field configuration of LHD, energetic particles from plasmas often hit some of the molybdenum chips of CMA. In this case, temperatures of these chips are not used in the evaluation.

The NB injection efficiency is estimated by normalizing the evaluated NB injection power by the output power of the acceleration power supplies. Here, the monitor signals of the power-supply outputs are acquired by CAMAC data acquisition system. The typical estimated injection efficiencies for three tangential NBIs during the 17th experimental campaign were 0.36 for NBI#1, 0.32 for NBI#2 and 0.38 for NBI#3.

(4) Motor-Generator (MG)

The MG is used to supply the pulsed power to the NBI and the ECH for LHD. The MG had generated 21,085 shots in this fiscal year and 550,973 shots since its construction. The operation time was 1,059 hours in this fiscal year and 25,584 hours in total. Under the annual inspection in this fiscal year, the following components were checked: oil in the MG, the brushes, vacuum circuit-breakers for 6.6kV or 18kV, field circuit-breakers, contactors for scherbius and liquid resistor, transformers for magnetization or scherbius, and protective relay. Unfortunately, the collector ring fell into disrepair. We polished a collector ring, and exchanged brushes.

4. Diagnostics Technology Division

This division makes preparations for the deuterium experiments for the LHD and support diagnostic devices. We are preparing several kinds of radiation measuring equipments to ensure the safety of the experiments.

We are measuring environmental radioactivity in the LHD building and neighboring areas in order to estimate the influence of the deuterium experiments in the future. We support the development and construction of the neutron diagnostic systems and its calibration system.

And we support operation and maintenance of the diagnostic devices such as FIR, Microwave Reflectometer, Thomson scattering diagnostic, HIBP and others. And in order to store the extremely huge data from these diagnostics, the data storage system is prepared for the next campaign.

We also carried out the preliminary vacuum leak tests on the several diagnostic devices.

Our principal tasks in this fiscal year are described in the below.

(1) Radiation Monitoring

In the LHD, deuterium experiments are planned. For comparison in the future, we are measuring and compiling data of environmental radioactivity in the LHD building and neighboring areas. We are providing maintenance for and using several radiation measuring equipment to measure environmental radioactivity as below.

(i) High-Purity Germanium (HPGe) Detector

Some samples of soil or pine needles from the site of NIFS are measured with the HPGe to search spectrum data and nuclide. Filters of the radiation gas monitors are also measured with it. And it is confirmed whether this detector operates correctly by using Co-60 once a month.

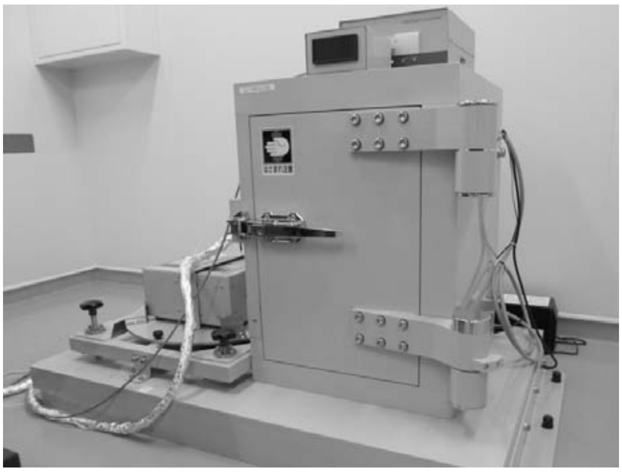

Fig. 19. High-purity germanium (HPGe) detector.

(ii) Gas Monitor

The radiation of the LHD room and the exhaust air are measured with the gas monitors using an ionization chamber. The data of the monitor can be checked and downloaded with a remote PC by LAN.

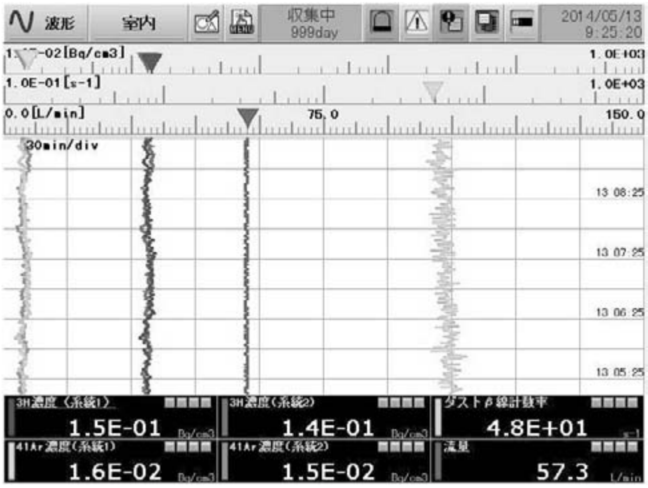

Fig. 20. Display of the room gas monitor on remote PC.

(iii) Water Monitor

We started to measure drain water from the LHD room and neighboring areas to simulate the control of drain water after the beginning of the deuterium experiments. The radiation of the drain water is checked with the water monitor device. The water is drained off after the confirmation of radiation.

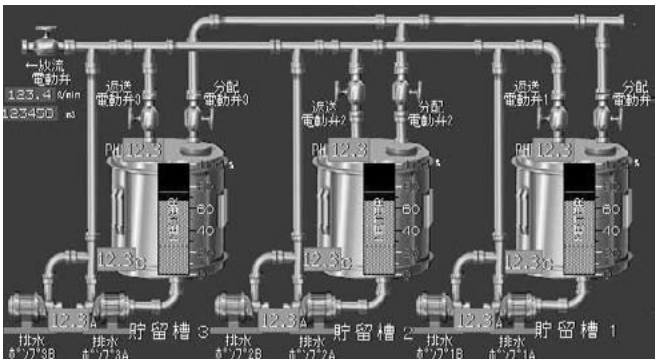

Fig. 21. Display of the drain control system.

(iv) Radiation Monitoring System Applicable to Fusion Experiment (RMSAFE)

More than 20 years has passed since the RMSAFE was constructed. Some parts are sometimes out of order and some parts are no longer available. Therefore, the RMSAFE was replaced in preparation for the deuterium experiments in this fiscal year.

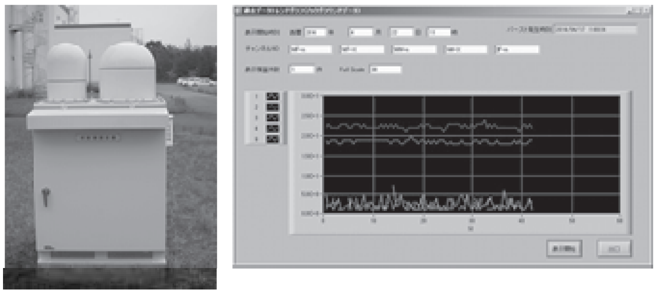

Fig. 22. Monitoring post repainted and monitor display.

(2) Neutron Diagnostics System

Neutron diagnostics system will consist of six detectors with different sensitivity and the digital-signal-processing system. The arrangement of these detectors is shown is Figure 23. Four detectors are located on 4-O and 10-O ports as the torus mid-plane. The others are on the top of LHD. The digital-signal processing systems are placed on the cellar of the device building and/or diagnostics room. The prototype unit of the digital-signal-processing system has been developed and the test operation has been carried out.

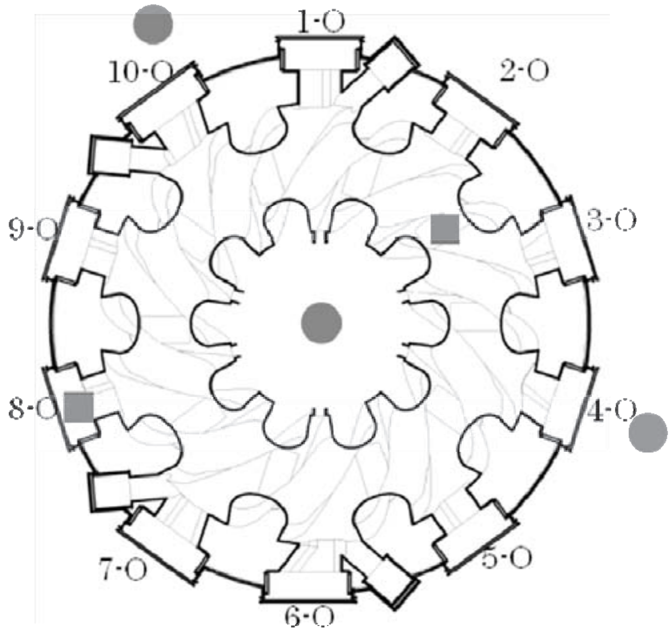

Fig. 23. Arrangement of the detectors and irradiated location on LHD.

For the purpose of efficiency calibration to those detectors, the remotely controlled source transfer system has been developed using O-gauge model train. The first assembly examination was conducted last year. Based on the result, this system has been improved. For example, the rail guide made by transparent polyvinyl chloride panel has been added for fall prevention, as shown in Figure 24, and the assembly way in the vacuum vessel has been improved. In the second assembly test, this system was constructed in the same manner as the calibration experiment, and the running test was done.

To check the detection efficiency of the neutron diagnostics system, two activation foil systems using air shutter have been developed. These irradiated locations are on 8-O and 2.5-L ports on LHD, respectively, as shown in Figure 23. To place the foils at close to plasma from atmospheric region, the port flange with a pipe keeping the vacuum has been designed.

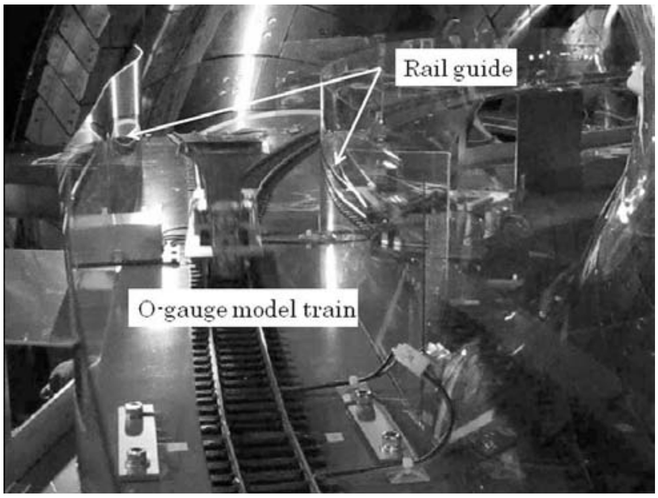

Fig. 24. Developed remotely controlled source transfer system.

(3) Operation and Maintenance of Diagnostics Device

The operation and the maintenance(for example, high voltage power supply, vacuum pumping system, supplied gas system, phase detection circuit, dehydrator, water cooling system etc.) were responsibly executed. And we support the reform and shield of the laser pass of FIR and Thomson scattering diagnostic for the deuterium plasma experiments.

(4) Development of a Detector for a Heavy Ion Beam Probe (HIBP) on LHD

The increase in signal intensity of the HIBP on the LHD is required to improve the precision of measurement. In this fiscal year, a test equipment of a new detector which consists of a scintillator and a photomultiplier tube aiming at the improvement in detection sensitivity was designed. The scintillator is inserted between the energy analyzer and the secondary beam detectors by using a linear motion feed through, and the scintillation light is detected by the photomultiplier tube installed in another port. The scintillator was tested by use of Au2+ beam with the energy of 5.042 MeV and 1.092 MeV, and the ion beam was successfully detected in both cases.

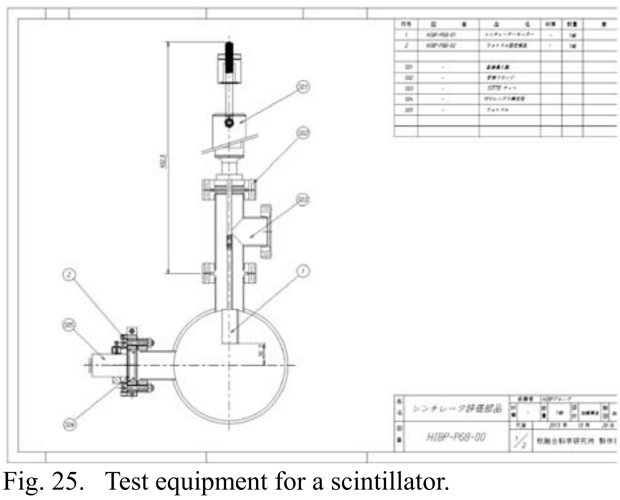

Fig. 25. Test equipment for a scintillator.

(5) LHD Data Storage System

For the LHD data storage system, we evaluated the free software "GlusterFS" that is a scale-out NAS file system. It is not so good in respect of the performance of read/write throughputs. On the other hand, we judged its reliability as sufficient. Consequently, we decided to continue using "GlusterFS" and to prepare for the 18th campaign to move the past data between 1st and 15th campaign from the old 16 RAIDs (gfs2 and IznaStor) to the new 4 RAIDs (GlusterFS). Thereby, we can replace the old RAIDs with the other new 4 RAIDs to store the data of the 18th campaign and cut off the total electricity consumption.

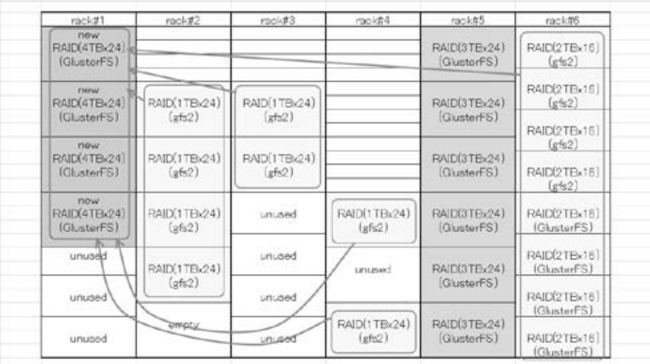

Fig. 26. Data Migration Procedure.

(6) Vacuum Leak Test Chamber in the Plasma Diagnostics Laboratories

The vacuum leak test chamber is maintained well and the preliminary vacuum leak tests were carried out on the several diagnostic devices to be used for the LHD plasma experiment with this chamber.

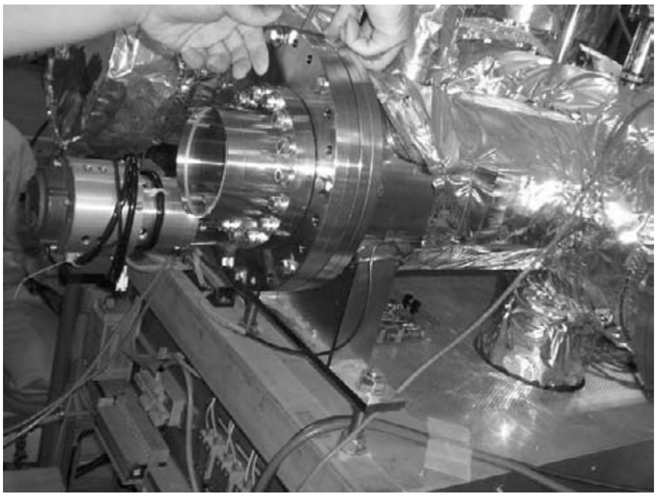

Fig. 27. Example of tested devices (window of the microwave reflectometer).

5. Control Technology Division

The Control Technology Division contributed to those important technological parts of the LHD, such as operation and management, and system development. And it contributed also to management of the network system. The work of the system operation and system management is as follows: operation of the cryogenic system and the power supply system for the super conducting coils, updating the central control system and cryogenic control system and coil quench detection system, and management of the network system. The work of the system development this year is as follows: development of a new simulation algorithm for the cryogenic system, system development of the control system for LHD, and others. Details of the activities in this division are described.

(1) Operation of LHD superconducting system

LHD cryogenic system operation was started on August 21 in the 17th experimental campaign, and helium gas was purified as usual. The coil cool-down was started on September 4, and it was completed on September 30. The number of steady-state operation days of the super conducting coils was 87 days. It was able to operate safely without serious trouble according to the experiment plan. The coil warm-up was started on December 26, and it was finished on January 17. The availability of the cryogenic system achieved 100%, and the total operation time was 3,575 hours in this campaign.

The first excitation of LHD in the 17th experimental campaign was started on September 30, and it was finished on December 25. The number of excitation times of LHD was 69, and the total operation time was 512 hours in this campaign. In these operations, the high voltage power supply for pulsed excitation was not used and the polarity switch device was used 24 times.

(2) Update of the LHD cryogenic control system

The cryogenics system gave a duplex operation by the CPCI system this year. The system total operating time was 356 days (8556 hours). The compressor total operating time was 148 days (3575 hours). It was a purification and cooling operation for the first time in CPCI system, but was able to drive without any trouble. There was one trouble by misconfigured operating steadily, but I was able to recover quickly.

(3) Update of the LHD central control system

The central control system requires high reliability. Since starting, 18 years have passed, and it become difficult to obtain maintenance parts. We decided to update these apparatuses in three years. The timing board, monitor system and backup server system were replaced with new ones last year. In this year, the third year, we updated the signal conditioners of more than 500 of the status monitoring system.

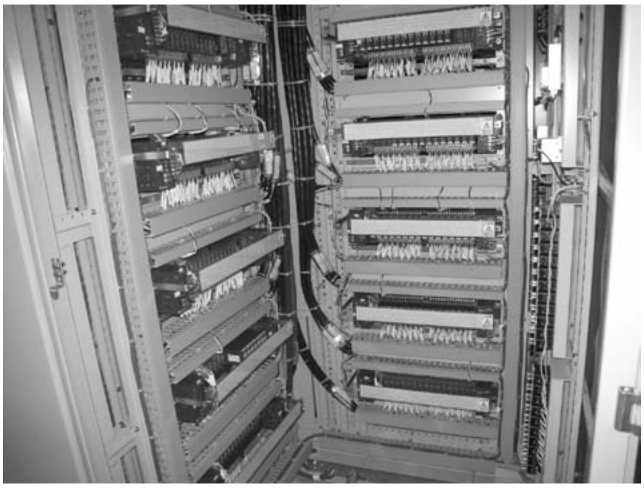

Fig. 28. Status monitoring system.

(4) Updating display system of helical coil balance voltage waveform

The LHD super conducting helical coil uses a display system of the balance voltage waveform to confirm its soundness visually. If normal conducting occurs partially, the balance voltage waveform will be unusual. But this system is very old (made in 1999), therefore, we updated it. Figure 29 shows a system block diagram. The computer acquires an amplified analog signal using “NI-USB6009” (14bit 48kS/s). And we made a program to display waveform by LabVIEW. Also, we made a remote supervision program that uses the LabVIEW “Shared Variable,” data in the host computer was transferred to a client computer. Image transfer using VNC causes is delayed but data transfer causes less delay. We displayed three kinds of 12bit analog signals very smoothly (sampling 20msec) using gigabit Ethernet. (Figure 30: screen displaying waveform)

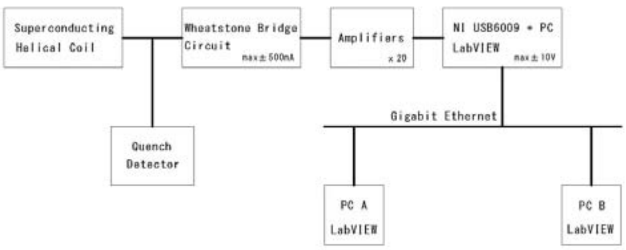

Fig. 29. System block diagram.

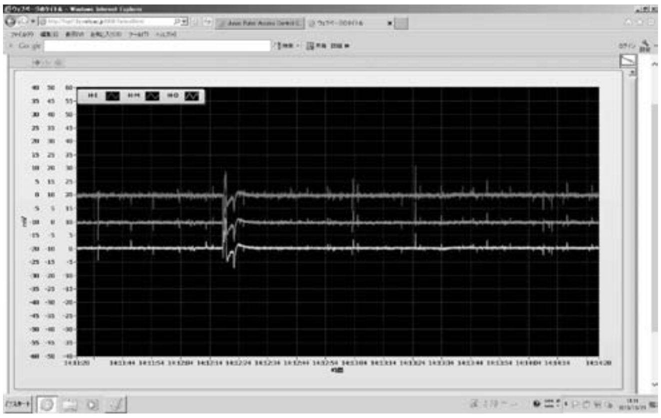

Fig. 30. Screen displaying waveform.

(5) Network management

The NIFS campus information networks consist of several clusters. We managed the Research Information Cluster (NIFS-LAN) and LHD Experiment Cluster (LHD-LAN).

(5.1) NIFS-LAN

NIFS-LAN is the network of general use, and covers the entire campus area. We have administrated the Routers, layer-2 / layer-3 switches, Mail server, SSL-VPN server, DNS server and DHCP server.

New contributions in FY 2013 are as follows:

(a) Renewed the edge switch system and introduced a new security system

The edge switches in a research building, an administration building, and an experimental building have been replaced with Apresia13200 layer-2 switch (Figure 31). The new security system which detects malware and quarantines computers has been introduced in NIFS-LAN. Its malware detection system monitors communications such as call-back by a malware and has the ability to stop communications once it detects an anomaly.

(b) Distributed the SEP version 12.1.4

Distribution of the Symantec Endpoint Protection (SEP) version 12.1.4, which covers Windows 8.1, Windows Server 2012 R2 and MacOS X 10.9.

(c) Upgrade the operating system of the SSL-VPN server

The operating system of the SSL-VPN server was upgraded in order to make Windows 8.1 and newer versions of security software available to remote access service users.

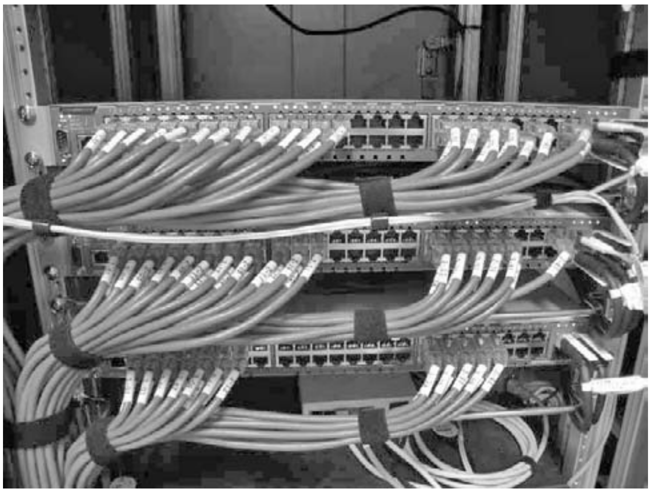

Fig. 31. The new NIFS-LAN edge switch.

(5.2) LHD-LAN

The LHD-LAN has been contributing to the LHD experiments since 1996. The new “LHD-LAN Core Switch System” has been renewed in the 2007-2008 fiscal years. The main part consists of two Cisco Catalyst 4507R multi-layer switches connected by 10 Gbps Ethernet, whose maximum throughput is over 210 million packets per second.

The main new contributions in FY 2013 are as follows:

(a) LHD Access gateway

We operate the gateway device MAG4610 made by Juniper Network Inc., which interconnects between the Research Information Cluster and the LHD Experimental Cluster. Because users increased, we increased licenses to 100 from 50. As daily business, we responded to users' inquiries, update the security policy, and other issues.

(b) Renewal of DNS servers

We updated four DNS servers, because the DNS servers had become old. A model is “PRIMERGY RX100 S7” (CPU: Xeon ES-1220 V2 @ 3.10GHz , Memory: 4GB) of Fujitsu Ltd. (See Figure 32) Failure resistance of new DNS servers was improved by RAID1 system and the dualization of the power supply. We adopted CentOS as its operating system, which is proven in NIFS.

Fig. 32. PRIMERGY RX100 S7.

(6) Updating the control systems for essential facilities attached to the LHD experiment

We have routinely received development requests about control systems from researchers, and have carried out every phase from consultation to implementation and maintenance.

For this fiscal year, our main task was to improve the functionality of the control system for essential facilities attached to the LHD plasma experiment, such as water-cooling device, fueling pellet injector and others. Another important task was to port the control applications of aging systems, which have been worked on since the plasma experiments started 17 years ago, into a new operating environment. Even though there are difficulties because some of them are currently running on ancient operating systems and/or we have to analyze the detailed specifications of the control systems developed by subcontracting without enough documents, it is going smoothly with the cooperation of all the concerned departments.

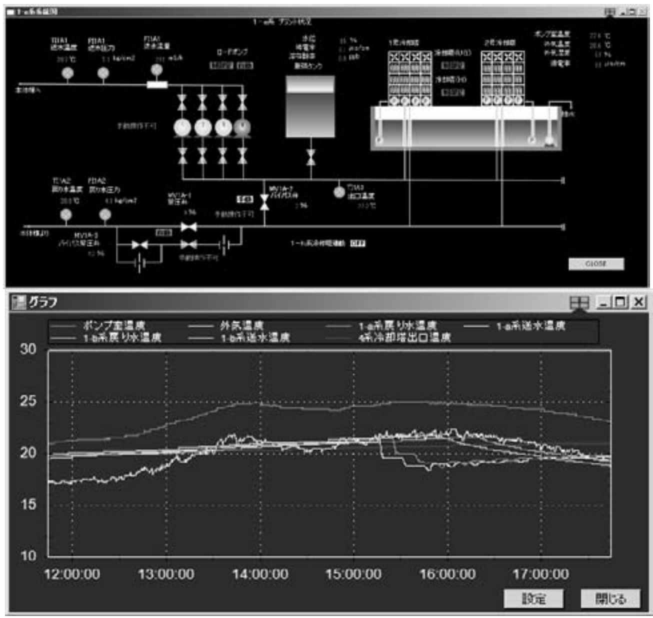

Fig. 33. Monitoring system for water-cooling device.

(7) Fabrication of remote control device using general-purpose I/O module

In LHD the demands for remote control are increasing. Therefore, we fabricated an inexpensive remote control device using a general-purpose I/O module. We used the I/O module with LAN port “LANX-I16” (digital input 16ch, digital output 16ch, analog input 4ch, and analog output 2ch). Controllable maximum load is 5A, maximum analog signal is 10V. This device has two solenoid valves and therefore enables control of compressed air ON/OFF. (Figure 34 Remote control device) Now, we are connecting vacuum gauges, a gate valve (compressed air drive) and a turbo-molecular pump to this device and we can operate these by remote control without problems.

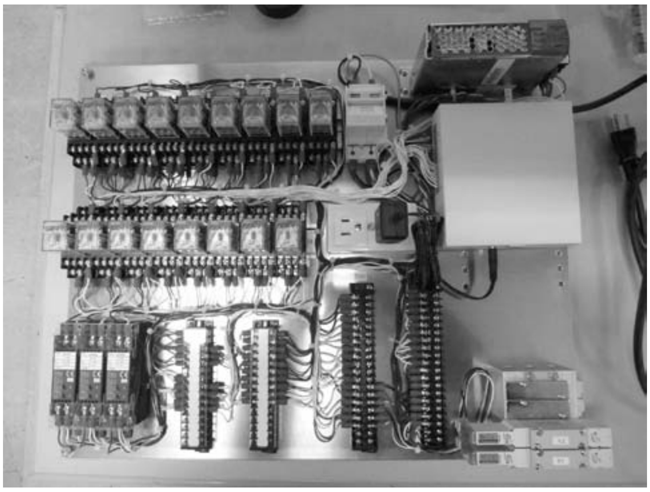

Fig. 34. Remote control device.

(8) Modeling and simulation of SHe loop of the TF structure (TFST) in ITER cryoplant by C-PREST

In the past, the dynamic simulation of the CEA (Commissariat a l'energie atomique et aux energies alternatives) test loop experiment to study ITER relevant supercritical helium (SHe) loop was carried out. We successfully validated the simulation model in C-PREST.

In 2013, we implemented modeling and simulation of the thermal-hydraulic behavior of a forced-flow SHe loop of TFST to investigate process control so to mitigate heat load from TFST. Figure 35 shows a schematic of the SHe loop of TFST, which consists of two heat exchangers (HXs) immersed in LHe reservoir, a circulation pump (CP), TFST composed of 18 modules and bypass valves for flow distribution. The simulation model has been modeled one TFST module. Accordingly, the characteristics of HXs, CP and valves were scaled down. Figure 36 shows the heat transfer to the LHe reservoir from HXs when rotational speed of the CP is controlled. By manipulating the rotational speed, the mass flow rate of SHe was changed, and the heat transfer to SHe loop from TFST was controlled. Therefore, the heat transfer to the LHe reservoir was suppressed.

In the future, we will implement the modeling and simulation of the SHe loop of the superconducting coils.

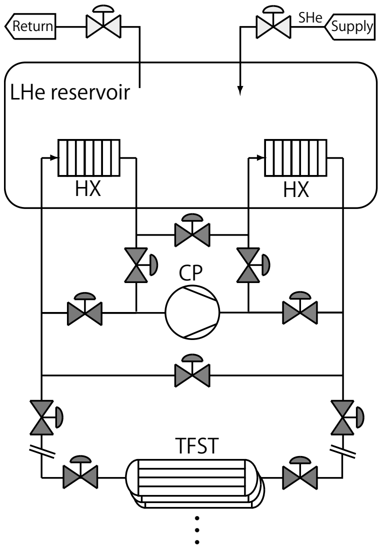

Fig. 35. Schematic of the TFST cooling loop.

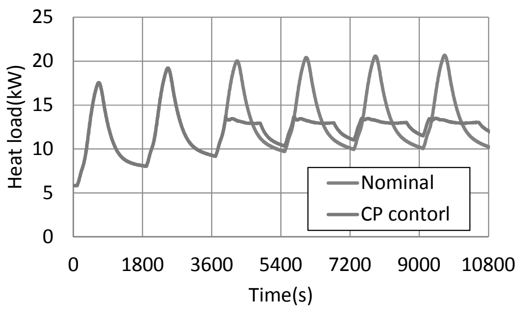

Fig. 36. Heat transfer to the LHe reservoir from the HXs.

6. Symposium on Technology

The Symposium on Technology was held March 13-14, 2014, at Freude in Inuyama city, Aichi Prefecture, Japan. It was hosted by the National Institute for Fusion Science (NIFS). There were 275 participants from many Japanese universities, national laboratories and technical colleges. In this symposium 48 oral presentations and 44 posters were presented in 5 technical groups. The 80 participants visited NIFS to see LHD. Figure 37 shows the opening ceremony.

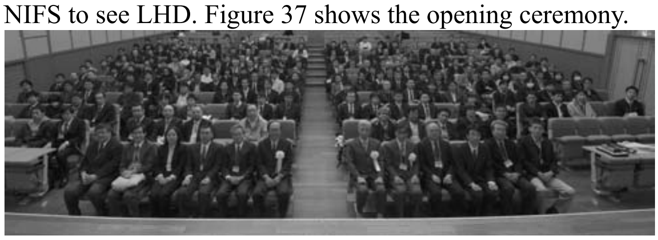

Fig. 37. A snapshot of the opening ceremony.